FDTD ANALYSIS OF TOP-HAT MONOPOLE ANTENNAS LOADED WITH RADIALLY LAYERED DIELECTRIC

K. Paran and M. Kamyab

Department of Electrical Engineering, K.N. Toosi University of Technology
Tehran, Iran, pkpkp@eetd.kntu.ac.ir and Kamyab@eetd.kntu.ac.ir

N. Ahmadi Tabatabaei

Department of Complementary Education, Tehran South Unit, Azad University
Tehran, Iran, natabaee@yahoo.co.uk

(Received: December 14, 2003 – Accepted in Revised Form: May 10, 2004)

Abstract Top-hat monopole antennas loaded with radially layered dielectric are analyzed using the finite-difference time-domain (FDTD) method**.** Unlike the mode-matching method (MMM) (which was previously used for analyzing these antennas) the FDTD method enables us to study such structures accurately and easily. Using this method, results can be obtained in a wide frequency band by performing only one time-domain simulation. For the FDTD modeling, the type of medium at each grid point is specified by a code. Also an efficient non-uniform meshing scheme and a novel perfectly matched layer (PML) are presented and used. The excitation signal can be chosen in the form of Gaussian pulse (GP) or sine carrier modulated by Gaussian pulse (SCMGP). These enable us to increase the accuracy of simulation and decrease the required memory and CPU time. Simulation results are presented in the form of graphical figures, which display the spatial variations in amplitude and phase of radiated field. Also, the FDTD computed input impedances of several top-hat monopole antennas are compared with those obtained by measurement. The agreement between computed and measured results is quite well.

Key Words FDTD Method, Top- Hat Monopole Antenna, Dielectric Loaded Antenna

چکیده نحوه و مزایای استفاده از روش تفاضل محدود در حوزه زمان (FDTD) برای بررسی آن دسته از آنتن های top-hat که دارای بارگذاری دی الکتریکی با لایه هایی در راستای شعاعی هستند، در این مقاله شرح داده می‌شود. بر خلاف روش تطبیق مدی (MMM) (که در گذشته برای تحلیل این آنتنها بکار گرفته شده است) با استفاده از روش FDTD می‌توان به آسانی و با دقتی بالا چنین ساختارهایی را بررسی نمود و در یک باند فرکانسی گسترده، نتایج مورد نظر را تنها با انجام یک شبیه سازی در حوزه زمان بدست آورد. در شیوه ای که در این پژوهش برای شبیه سازی FDTD بکار گرفته شده است، نوع محیط در هر نقطه از شبکه با استفاده از یک کد مشخص می‌گردد. همچنین از شبکه بندی غیر یکنواخت و نوعی لایه جاذب با تطبیق کامل(PML) استفاده می شود. سیگنال تحریک نیز بشکل پالس نرمال (GP) یا پالس نرمال مدوله شده با تابع سینوسی (SCMGP) اختیار می‌گردد. این تدابیر موجب افزایش دقت و کاهش حافظه و زمان مورد نیاز برای شبیه سازی می‌شوند. نتایج شبیه سازی ها به کمک نمایه هایی گرافیکی که تغییرات دامنه و فاز میدان تابشی را در اطراف آنتن نمایش می‌دهند و منحنی هایی که نشان دهنده امپدانس ورودی آنتن هستند، ارائه شده اند. مقادیر محاسبه شده امپدانس ورودی با مقادیر اندازه گیری شده مقایسه گشته اند. این مقادیر به میزان زیادی با یکدیگر مطابقت دارند.

1. INTRODUCTION

Since the presentation of the finite-difference time-domain (FDTD) method in 1966 [1] this method has found applications in almost all fields of electromagnetics. Simulation of electromagnetic phenomena such as radiation [2], scattering [3,4] penetration [5], absorption [6], coupling and interference [7,8] and analysis of different kinds of guiding [9,10] and radiating [11] structures show the unique capabilities of the FDTD method and its superiority over other conventional

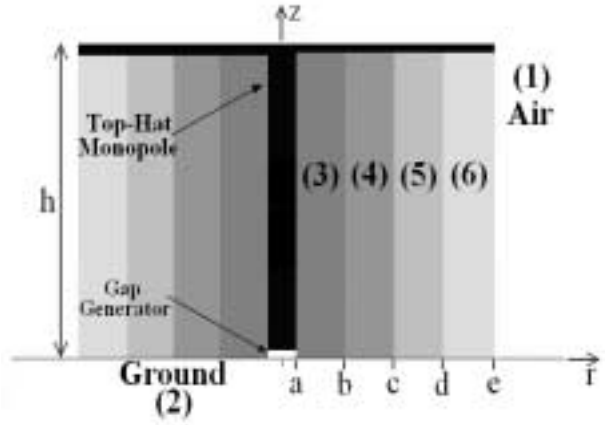

Figure 1. Top-hat monopole antenna loaded with radially layered dielectric.

methods.

In the case of radiating structures, this method enables us to allow for all structural details, materials with different electromagnetic characteristics and media, structures and objects around antenna. Also the FDTD method provides the ability to consider non-sinusoidal excitations (e.g. pulse signals). Therefore, it is possible to calculate the characteristics of antenna in a wide frequency band only by performing the time-domain simulation once and using the Fourier transform.

Pioneering researches by Smith et al. are among the most significant works that have been carried out in this field. In their works, perfectly conducting cylindrical and conical monopoles [12], Wu-King resistive monopole [13], an optimized conical antenna for pulse radiation [14], several broadband loaded monopoles [15], and insulated linear antenna in lossy media [16] were analyzed by 2-D cylindrical FDTD method. Using Gaussian pulse (GP) or differentiated Gaussian pulse (DGP) as excitation signal, the process of radiation by these antennas was studied and characteristics of antennas in time and frequency domains were computed with high accuracy. Researches made by Shum and Luk about two kinds of ring dielectric resonator antennas [17,18] are also worthy of attention. In their works, the excitation signal was considered in the form of GP or cosine carrier modulated by Gaussian pulse (CCMGP) and characteristics of antennas were obtained in a specified frequency band using the Fourier transform.

In the present research, the problem of top-hat monopole antenna with homogeneous and inhomogeneous dielectric loading (Figure 1) is studied using the FDTD method in cylindrical coordinates taking the rotational symmetry into consideration. Top-hat loading of an electrically small vertical monopole antenna modifies the current distribution on the antenna in such a way as to decrease the radiation Q and increase the radiation resistance of the antenna [19]. On the other hand, the dielectric loading, in addition to making the electrically small antenna self-resonant, makes the structure much more mechanically robust. The combination of top hat loading with the use of low-loss loading materials can, therefore, produce a broadband electrically small self–resonant antenna with high radiation efficiency [20,21].

In previous researches, the mode-matching method (MMM) was used for analyzing these antennas. Due to limited number of modes, the resultant expressions for field components in different sections (especially in gap region) are of limited accuracy. In addition, the MMM is a frequency-domain method and in order to obtain results in a frequency band, the MMM analysis must be carried out for different frequencies separately which takes a long CPU time. Moreover, for top-hat antennas with more than two dielectric layers, the MMM analysis is a very difficult task (if not impossible). On the contrary, the FDTD method enables us to analyze these structures accurately and easily (by performing only one time-domain simulation for each structure).

In this article, the key points of FDTD simulation in the case of above mentioned problem are described, including subjects such as meshing scheme, mesh truncation technique and excitation scheme. Simulation results are produced in the form of graphical figures, which display the spatial variations in amplitude and phase of radiated field. Also, the FDTD computed input impedances of several top-hat monopole antennas are presented by some curves and compared with those obtained by measurement.

2. FDTD SIMULATION

2.1 FDTD Formulation The FDTD formulation of this problem is obtained by taking the following steps:

(a) Maxwell's curl equations should be expressed in cylindrical coordinates taking the rotational symmetry of structure and excitation $(\partial/\partial\varphi \equiv 0)$ into account. The gap-generator in Figure 1 only excites the rotationally symmetric TM modes (E_r, E_z, H_φ) [20,21]. For future applications, the general case of anisotropic media $(E_r, E_z, H_{\varphi r}, H_{\varphi z})$ is assumed.

(b) After the discretization of time and space (Figure 2), the temporal and spatial derivatives must be replaced with the central difference approximations.

For example, it can be shown that the FDTD equation for E_z component is:

$$E_z(i,j^+,n+0.5) = C_{E_z1}(i,j^+)E_z(i,j^+,n-0.5) + C_{E_z2}(i,j^+)\left(r_p(i)H_\varphi(i^+,j^+,n) - r_m(i)H_\varphi(i^-,j^+,n)\right) \quad (1)$$

where the coefficients $C_{E_z1}(i,j^+)$, $C_{E_z2}(i,j^+)$, $r_p(i)$ and $r_m(i)$ are:

$$C_{E_z1}(i,j^+) = \frac{\frac{\varepsilon_z(i,j^+)}{\Delta t} - \frac{\sigma_z(i,j^+)}{2}}{\frac{\varepsilon_z(i,j^+)}{\Delta t} + \frac{\sigma_z(i,j^+)}{2}} \quad (2a)$$

$$C_{E_z2}(i,j^+) = \frac{1}{\frac{\varepsilon_z(i,j^+)}{\Delta t} + \frac{\sigma_z(i,j^+)}{2}} \quad (2b)$$

$$r_p = \frac{2r(i^+)}{r^2(i^+) - r^2(i^-)} \quad (3a)$$

$$r_m = \frac{2r(i^-)}{r^2(i^+) - r^2(i^-)} \quad (3b)$$

Using Equation 1, the electric and magnetic characteristics $(\varepsilon_z(i,j^+), \sigma_z(i,j^+),$ etc) and the

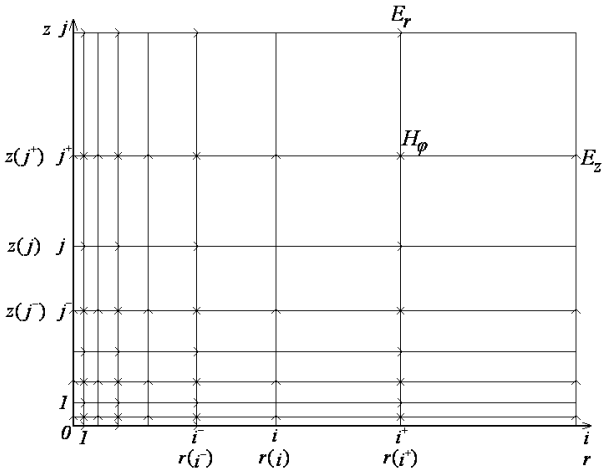

Figure 2. Spatial discretization for two-dimensional problem with rotational symmetry.

FDTD coefficients ($C(i,j)$'s), which are real numbers, must be considered, calculated and saved in memory for all grid points (all (i,j)'s). This needs a massive amount of memory. In this simulation, these values are considered, calculated and saved in memory only for media and materials that exist in the computational space. The only parameter that is allocated to all grid points is a code (an integer number) that specifies the type of medium at each point. Therefore, Equation 1 can be expressed in the following form:

$$E_z(i,j^+,n+0.5) = C_{E_z1}(m_e)\,E_z(i,j^+,n-0.5) + C_{E_z2}(m_e)\left(r_p(i)H_\varphi(i^+,j^+,n) - r_m(i)\,H_\varphi(i^-,j^+,n)\right) \quad (4a)$$

$$m_e = m_e(i,j^+) \quad (4b)$$

$$C_{E_z1}(m_e) = \frac{\frac{\varepsilon_z(m_e)}{\Delta t} - \frac{\sigma_z(m_e)}{2}}{\frac{\varepsilon_z(m_e)}{\Delta t} + \frac{\sigma_z(m_e)}{2}} \quad (5a)$$

$$C_{E_z2}(m_e) = \frac{1}{\frac{\varepsilon_z(m_e)}{\Delta t} + \frac{\sigma_z(m_e)}{2}} \quad (5b)$$

$$m_e = 1, 2, ..., n_{m_e}$$

where n_{m_e} is the number of media and materials in the computational space and m_e is the code that specifies the type of medium. In this manner, much less memory will be needed for simulation.

2.2 Meshing For choosing the meshing scheme in this simulation, it is necessary to consider some points:

(a) In order to obtain an acceptable accuracy, the radiating structure should be modeled with fine cells ($\Delta l \leq 0.02\lambda_{min}$ [1]). On the other hand, the FDTD simulation of electromagnetic radiation from antenna up to far zone needs a grid with large dimensions. In such a grid, coarse cells should be used in order to keep the required memory and CPU time below a reasonable limit.

(b) Since the wavelength in dielectrics is shorter than that in air, finer cells must be used for modeling these parts.

(c) In some cases, only a little difference (even in the order of a fraction of cell width) between dimensions of FDTD model and dimensions of actual structure may cause sensible deviations in obtained values of some characteristics such as input impedance of radiating structure. Therefore, dimensions of FDTD model should be as close as possible to dimensions of actual structure.

Based on the above-mentioned points, in this simulation an efficient non-uniform meshing scheme is used. In this scheme, the computational space is divided into sections with specified lengths along both radial and vertical directions, according to the geometry of structure. For example, Figure 3 shows the division of computational space when antenna is loaded with four dielectric layers. The values of cell width at the edges of sections and the extremum values of cell width in each section are also chosen so that each section of the structure can be modeled with a proper resolution (Figure 4). Then for each section, the number of cells and the width of each cell are calculated so that the length of the section will be "exactly" equal to the specified value and at the same time variations in cell width, from one edge

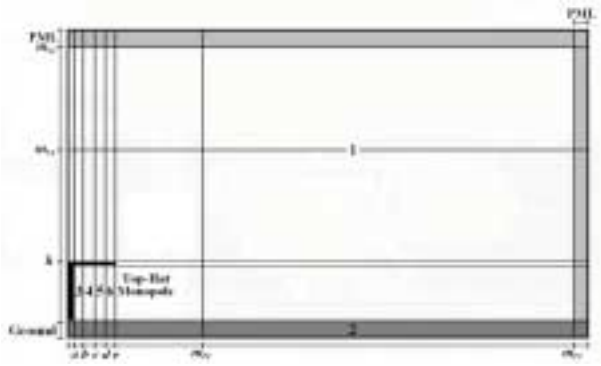

Figure 3. Division of computational space for the problem of top-hat monopole antenna with radially layered dielectric (figure is not drawn to scale).

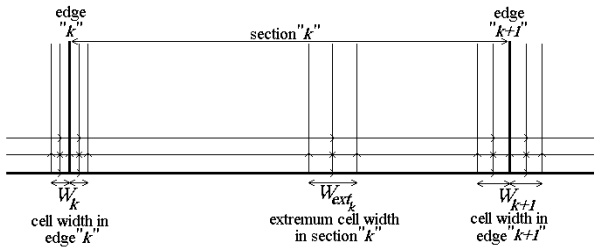

Figure 4. Meshing of an arbitrary section.

of the section to the other, will take place in a smooth and gradual manner. It is obvious that there is not any sudden change in cell width while crossing the common edge of two adjacent sections.

Using this scheme, dimensions of the obtained model will be "exactly" equal to those of structure. Besides, it is possible to use fine cells wherever in mesh which are necessary and use coarse cells in other parts, without facing any sudden change in cell width throughout the mesh. In this manner, the required memory and CPU time can be considerably reduced.

2.3 Mesh Truncation In this simulation, a perfectly matched layer (PML) with a simple formulation is implemented for truncating the computational space. Values of the electric and magnetic characteristics at those parts of the

[1] λ_{min} is the shortest wavelength in the spectrum that has an intensity worthy of consideration.

absorbing layer that are adjacent to a specific medium must satisfy the following conditions:

$$\begin{cases} |R_{pm}| = 0 : \forall \theta_i \\ \alpha_p = \alpha \end{cases} \Leftrightarrow \begin{cases} Z_p = Z_m \\ \beta_p = \beta_m \\ \alpha_p = \alpha \end{cases} \quad (6)$$

where subscripts "m" and "p" stand for "medium" and "PML" respectively, R_{pm} is the reflection from medium-PML interface, θ_i is the incidence angle, α and β are attenuation and phase constants and Z is the intrinsic impedance. After some mathematical operations, the following relations can be obtained for the electric and magnetic characteristics of the PML:

$$\begin{cases} \rho_p = Z_m \alpha \\ \mu_p = \mu_m \\ \sigma_p = Y_m \alpha \\ \varepsilon_p = \varepsilon_m \end{cases} \quad (7)$$

Subscripts "r" and "z" of ρ, μ, σ and ε are omitted in (7). The value of α should be smoothly increased from inner cells (sub-layers) of the PML towards outer ones:

$$(\alpha)_q = (\alpha)_{max} \left(\frac{q}{n_p} \right)^{o_p} \qquad q = 1, 2, ..., n_p \quad (8)$$

In (8), n_p is the number of cells along the width of absorbing layer (number of sub-layers) and o_p is the order of increase (o_p = 1 linear, o_p = 2 parabolic, etc).

2.4 Excitation Scheme The excitation source is a delta-gap-generator between top-hat monopole and ground plane (Figure 1) and it is possible to choose the excitation signal in the form of GP or sine carrier modulated by Gaussian pulse

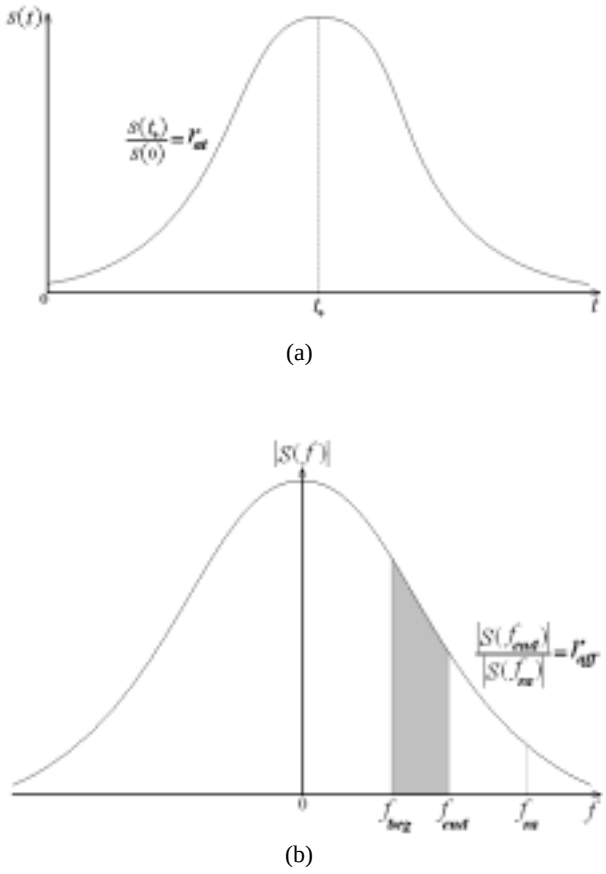

Figure 5. Gaussian pulse: (a) Temporal variations and (b) Spectral density.

(SCMGP). In order to have an excitation signal in the form of GP, with temporal variations and spectral density shown in Figure 5, the following equation should be used:

$$s(t) = s(n\Delta t) = \exp\left(-(nm_{exp} - s_{exp})^2\right) \quad (9)$$

$$m_{exp} = \pi \Delta t \sqrt{\frac{f_{ra}^2 - f_{end}^2}{\ln(r_{aff})}} \quad (10a)$$

$$s_{exp} = \sqrt{\ln(r_{at})} \quad (10b)$$

where f_{end} is the highest frequency in the

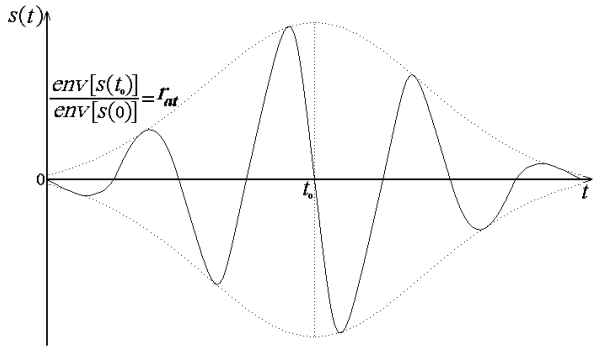

(a)

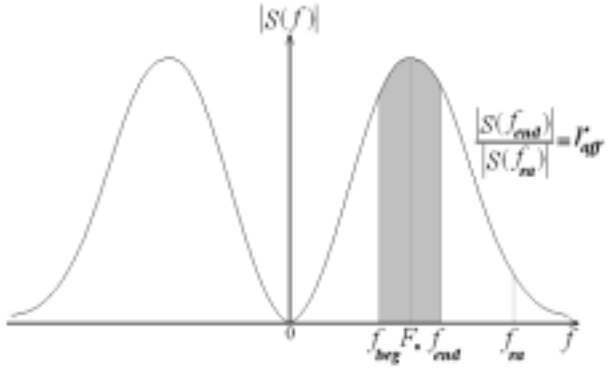

(b)

Figure 6. Sine carrier modulated by Gaussian pulse: (a) Temporal variations. (b) Spectral density.

frequency band of interest and f_{ra} is an arbitrary frequency which is chosen in order to have a spectral density r_{aff} times less than that of f_{end}. r_{at} is the ratio between the maximum value and the starting value of signal. In this simulation, the values of f_{ra}, r_{aff} and r_{at} are considered to be $2f_{end}$, 10^{-2} and 10^{-4} respectively.

In order to have an excitation signal in the form of SCMGP, with temporal variations and spectral density shown in Figure 6, the following equation should be used:

$$s(t) = s(n\Delta t)$$

$$= \sin(nm_{sin} - s_{sin}) \exp\left(-(nm_{exp} - s_{exp})^2\right) \quad (11)$$

$$m_{sin} = 2\pi F_0 \Delta t \qquad s_{sin} = \pi p \quad (12)$$

$$m_{exp} = \frac{\Delta t}{\sqrt{2}s_d} \qquad s_{exp} = \frac{pT_0}{2\sqrt{2}s_d} \quad (13)$$

$$F_0 = \frac{f_{end} + f_{beg}}{2} \qquad T_0 = \frac{1}{F_0} \quad (14)$$

$$s_d = \frac{1}{\pi}\sqrt{\frac{\ln(r_{aff})}{2(f_{ra} - f_{end})(f_{ra} - f_{beg})}} \quad (15)$$

$$p = \text{int}\left(\frac{2s_d}{T_0}\sqrt{2\ln(r_{at})}\right) + 1 \quad (16)$$

where f_{beg} is the lowest frequency in the frequency band of interest and r_{at} is the ratio between the maximum value and the starting value of signal's envelope. SCMGP unlike the ordinary GP (or even CCMGP) has very small low frequency content. This reduces the settling time and consequently the required CPU time. Signals such as DGP always have the same spectral distribution relative to the frequency of peak (f_p). For example, the 50% bandwidth of DGP is always between $0.319\,f_p$ and $1.922\,f_p$. On the contrary, by using SCMGP it is possible to concentrate or spread the spectrum density around the main frequency arbitrarily. Therefore, we can raise the spectrum density at a specified frequency band and reduce it at other frequencies and consequently increase the accuracy of calculations for the frequency band of interest.

In this simulation, the input voltage and the input current of top-hat antenna are found at each time step. Using the discrete Fourier transform, the values of these parameters can be obtained at different frequencies. In this manner, the impedance of top-hat antenna is calculated in the frequency band of interest. Also, the Fourier transforms of field components are obtained at each grid point in order to find the spatial distributions of amplitude and phase of radiated

wave at a specified frequency.

3. SIMULATION RESULTS

In this section, some of the results, which are obtained by FDTD simulations, are presented for the cases of loaded and unloaded top-hat monopole antennas. The computed values are compared with the experimental results (presented in [20] and [21]) in order to verify the accuracy of FDTD simulations.

3.1 Unloaded Top-Hat Monopole Antenna

Figure 7 shows the computed and measured input impedances of an unloaded top-hat monopole antenna. The dimensions of this antenna are: a = 0.119 cm, e = 3.87 cm and h = 3.175 cm. It can be observed that the FDTD results are in good

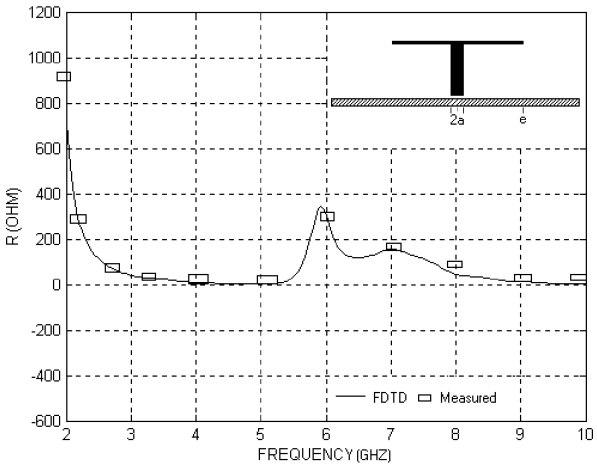

(a)

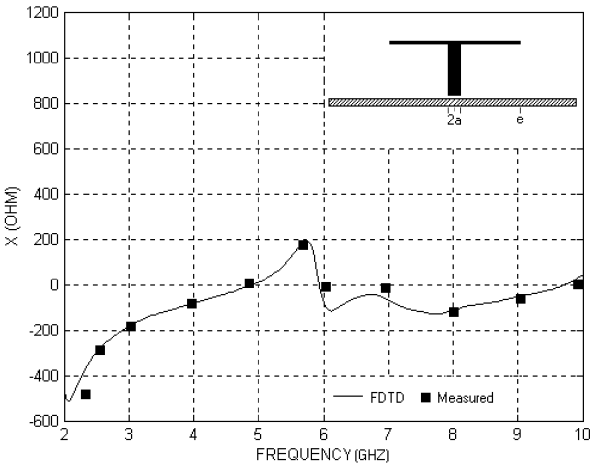

(b)

Figure 7. Comparing FDTD computed input impedance of unloaded top-hat monopole antenna with those obtained by measurement [20] over the frequency band f = 2 – 10 GHz. The dimensions of the antenna are: a = 0.119 cm, e = 3.87 cm and h = 3.175 cm.

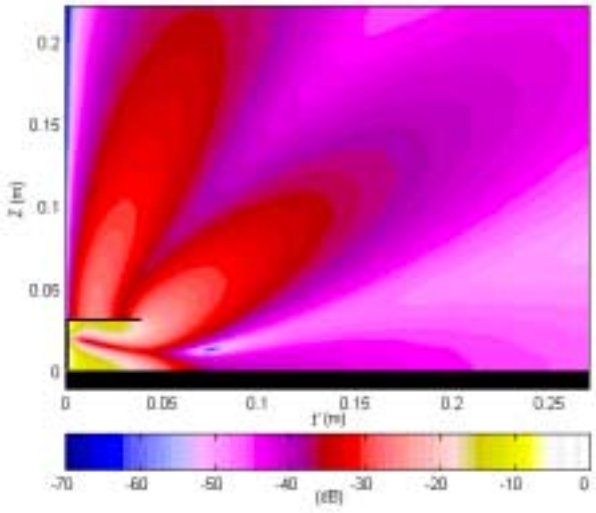

(a)

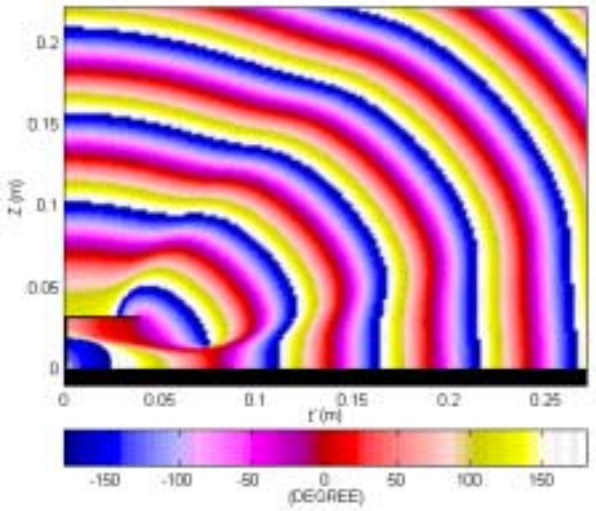

(b)

Figure 8. Spatial variations in (a) amplitude and (b) phase of radiated field (H_φ component) at 6GHZ. The parameters are the same as in Figure 7.

agreement with those obtained by measurement. The spatial variations in amplitude and phase of radiated field (at 6GHz) are shown in Figure 8 (a and b).

3.2 Plexiglass-Loaded Top-Hat Monopole Antenna

In Figure 9, the computed and measured input impedances of a plexiglass-loaded top-hat monopole antenna are shown. The dimensions of this antenna are equal to those of the unloaded antenna in previous subsection. Estimates

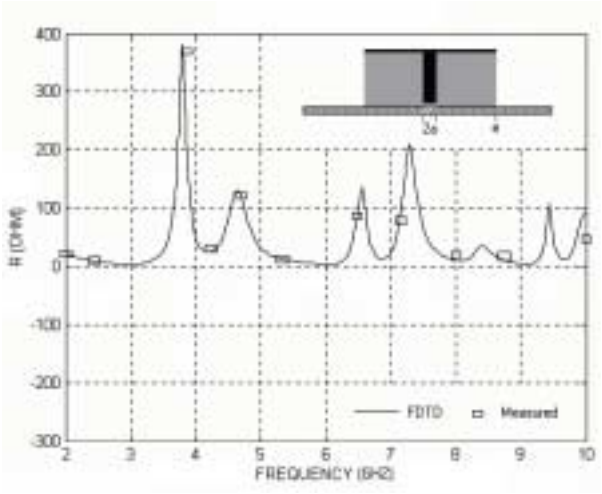

(a)

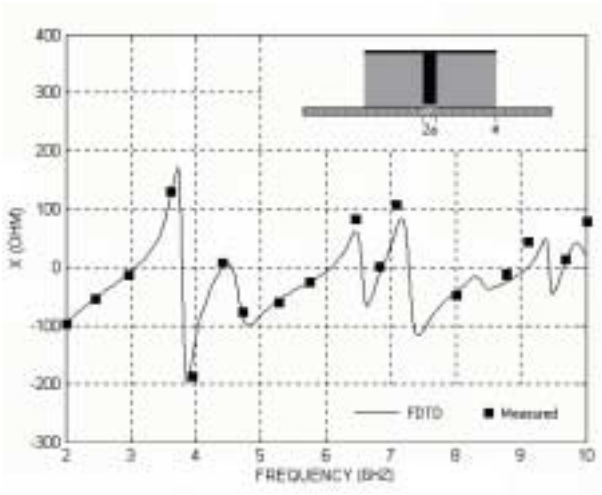

(b)

Figure 9. Comparing FDTD computed input impedance of plexiglass-loaded top-hat monopole antenna (ε_{re} = 2.56, σ = 0.01S/m), with those obtained by measurement [20] over the frequency band f = 2 – 10 GHz. The dimensions are the same as in Figure 8.

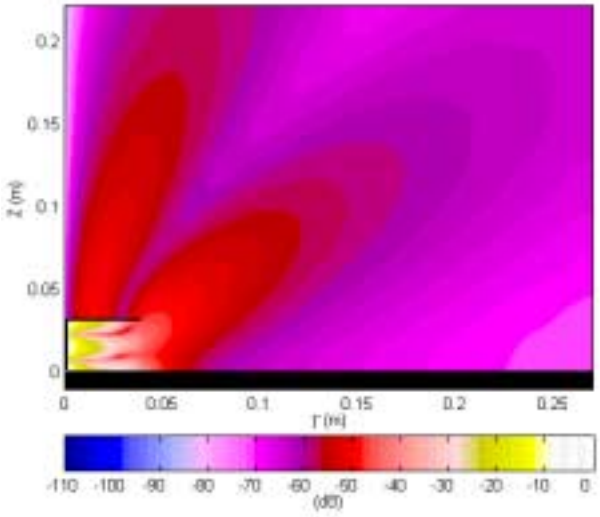

(a)

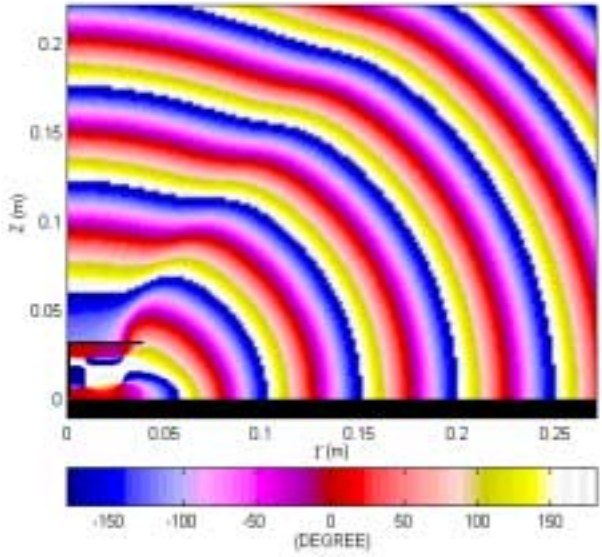

(b)

Figure 10. Spatial variations in (a) amplitude and (b) phase of radiated field (H_φ component) at 6GHz. The parameters are the same as in Figure 9.

of ε_{re}=2.56 and σ = 0.01S/m were used for the plexiglass in the FDTD computations over the 2-10GHz range. The agreement between computed and measured results is quite well. Figure 9 also shows the strong resonant behavior of $Z_{in}(f)$ induced by the plexiglass, as compared to the unloaded case in Figure 7. Within the dielectric, the internal path length of the stem and top hat ranges from $0.747\lambda_d$ (at 2GHz) to $3.73\lambda_d$ (at 10GHz). Dielectric loading is used to modify Z_{in} by increasing the apparent electrical size of the structure. Figure 10 shows the spatial variations in amplitude and phase of radiated field around this antenna (at 6GHz).

3.3 Teflon-Loaded Top-Hat Monopole Antenna A teflon-loaded top-hat monopole antenna was also studied. The dielectric loading of this antenna is inhomogeneous as teflon is placed only in regions 3 and 4 (Figure 1). The parameters of this antenna are: a = 0.2381cm, c = 1.27 cm, e = 3.81 cm, h = 3.2 cm, $\varepsilon_{re3} = \varepsilon_{re4}$ = 2.1 and $\varepsilon_{re5} = \varepsilon_{re6}$ = 1. The computed and measured input impedances of this antenna are shown in Figure 11. It can be observed that the computed results are in excellent agreement with the experimentally determined results.

3.4 Top-Hat Monopole Antenna Loaded with Four Dielectric Layers For top-hat monopole antennas with more than two dielectric layers, the MMM analysis is a very difficult task (if not impossible). On the contrary, in FDTD analysis the number of dielectric layers has no influence on complexity of simulation and such antennas can be easily analyzed. Here, a top-hat monopole antenna with four dielectric layers is considered. The parameters of this antenna are: a = 0.119 cm, b = 0.9525 cm, c = 1.905 cm, d = 2.8575 cm, e = 3.81 cm, h = 3.175 cm, ε_{re3} = 5, ε_{re4} = 4, ε_{re5} = 3 and ε_{re6} = 2. Figure 12 shows the impedance curves of this antenna in the frequency band of 200-1600MHz. The spatial variations in amplitude and phase of radiated field around this antenna (at 900MHz) are shown in Figure 13.

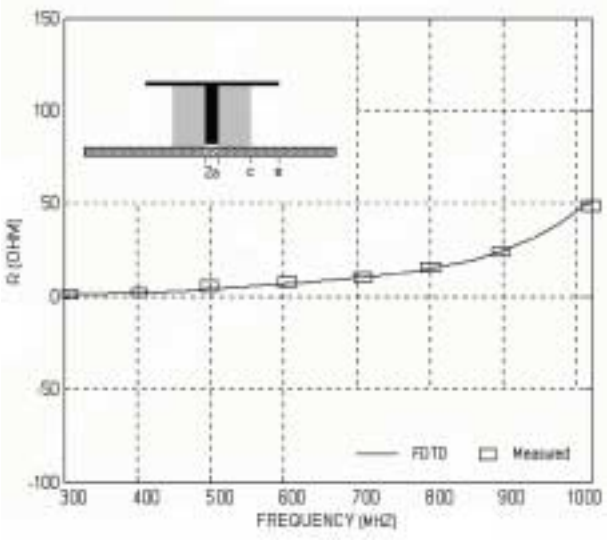

(a)

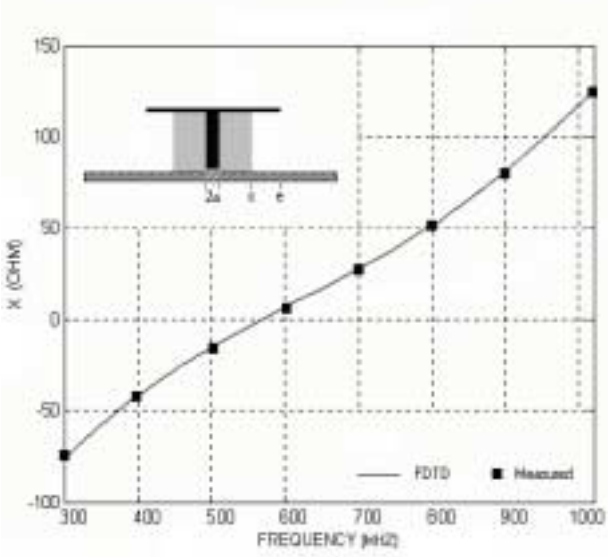

(b)

Figure 11. Comparing FDTD computed input impedance of teflon-loaded top-hat monopole antenna, with those obtained by measurement [21] over the frequency band f = 300 – 1000 MHz. The parameters of the antenna are: a = 0.2381 cm, c = 1.27 cm, e = 3.81 cm, h = 3.2 cm, $\varepsilon_{re3} = \varepsilon_{re4}$ = 2.1 and $\varepsilon_{re5} = \varepsilon_{re6}$ = 1.

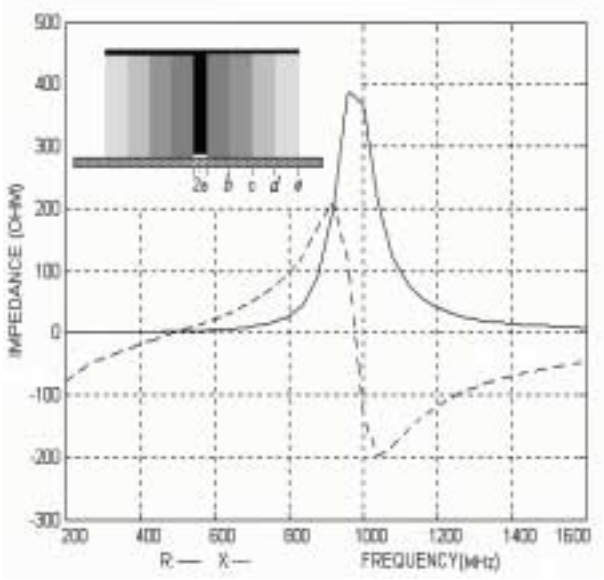

Figure 12. Input impedance of top-hat monopole antenna loaded with four dielectric layers (ε_{re3} = 5, ε_{re4} = 4, ε_{re5} = 3 and ε_{re6} = 2). The dimensions of the antenna are: a = 0.119 cm, b = 0.9525 cm, c = 1.905 cm, d = 2.8575 cm, e = 3.81 cm and h = 3.175 cm.

The FDTD analysis of each top-hat antenna requires about 20min of CPU time (using an 800MHz CPU), but the same analysis by MMM takes approximately 100 min, because the MMM analysis must be separately carried out for each frequency.

4. CONCLUSIONS

In this paper, top-hat monopole antennas with homogeneous and inhomogeneous dielectric loading were analyzed using the FDTD method in cylindrical coordinates taking the rotational symmetry into consideration. To increase the accuracy and convenience of simulation, some measures were taken:

(a) The electric and magnetic characteristics and the FDTD coefficients are considered, calculated and saved in memory only for media and materials which exist in the

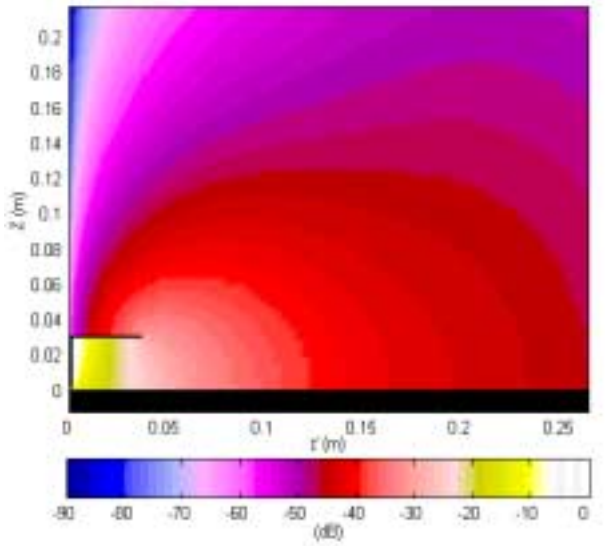

(a)

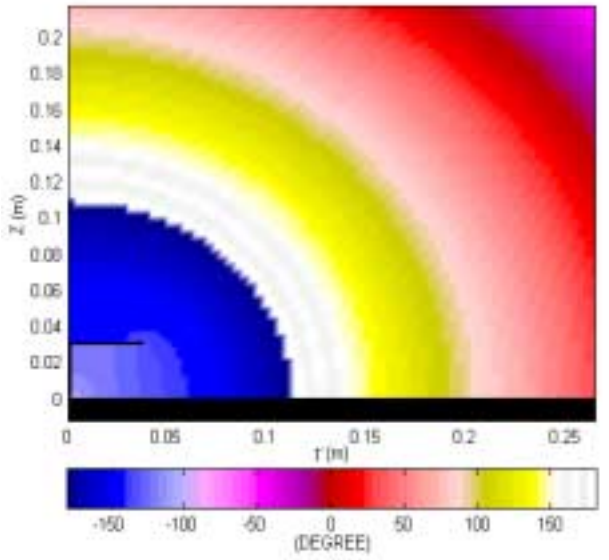

(b)

Figure 13. Spatial variations in (a) amplitude and (b) phase of radiated field (H_φ component) at 900MHz. The parameters are the same as in Figure 12.

computational space (not for all grid points). The only parameter that is allocated to all grid points is a code that specifies the type of medium at each point.

(b) Using an efficient non-uniform meshing scheme, structures can be accurately modeled i.e. dimensions of the obtained models will be "exactly" equal to those of structures. Besides, it is possible to use fine cells wherever in mesh which are necessary and use coarse cells in other parts, without facing any sudden change in cell width throughout the mesh.

(c) A novel PML was used which has a simple formulation and can be easily adapted for different applications.

(d) In simulations, it is possible to choose the excitation signal in the form of GP or SCMGP.

Simulation results were presented in the form of graphical figures, which display the spatial variations in amplitude and phase of radiated field. Also, the FDTD computed input impedances of several top-hat monopole antennas are presented by some curves and compared with those obtained by measurement. The agreement between computed and measured results is quite well, which shows the high accuracy of FDTD simulations.

5. REFERENCES

1. Yee, K. S., "Numerical Solution of Initial Boundary Value Problems Involving Maxwell's Equations in Isotropic Media", ***IEEE Trans. Antennas Propagat.***, Vol. AP-14, No. 3, (1966), 302-307.
2. Cummer, S. A., "Modeling Electromagnetic Propagation in the Earth-Ionosphere Waveguide", ***IEEE Trans. Antennas Propagat.***, Vol. 48, No. 9, (2000), 1420-1429.
3. Taylor, C. D., Lam, D. H. and Shumpert, T. H., "Electromagnetic Pulse Scattering in Time-Varying Inhomogeneous Media", ***IEEE Trans. Antennas Propagat.***, Vol. AP-17, No. 5, (1969), 585-589.
4. Merewether, D. E., "Transient Currents Induced on a Metallic Body of Revolution by an Electromagnetic Pulse", ***IEEE Trans. Electromagn. Compat.***, Vol. EMC-13, No. 2, (1971), 41-44.
5. Taflove, A., "Application of the Finite-Difference Time-Domain Method to Sinusoidal Steady-State Electromagnetic-Penetration Problems", ***IEEE Trans. Electromagn. Compat.***, Vol. EMC-22, No. 3, (1980), 203-209.
6. Taflove, A. and Brodwin, M. E., "Computation of the Electromagnetic Fields and Induced Temperature within a Model of the Microwave-Irradiated Human Eye", ***IEEE Trans. Microwave Theory Tech.***, Vol. MTT-23, No. 11, (1975), 888-896.
7. Holland, R., Simpson, L. and Kunz, K., "Finite - Difference Analysis of EMP Coupling to Lossy Dielectric Structures", ***IEEE Trans. Electromagn. Compat.***, Vol. EMC-22, No. 3, (1980), 203-209.
8. Holland, R. and Simpson, L., "Finite-Difference Analysis of EMP Coupling to Thin Struts and Wires", ***IEEE Trans. Electromagn. Compat.***, Vol. EMC-23, No. 2, (1981), 88-97.
9. Gwarek, W. K., "Computer Aided Analysis of Arbitrarily-Shaped Coaxial Discontinuities", ***IEEE Trans. Microwave Theory Tech.***, Vol. 36, No. 2, (1988), 337-342.
10. Zhang, X. and Mei, K. K., "Time-Domain Finite-Difference Approach to the Calculation of the Frequency-Dependent Characteristics of Microstrip Discontinuities"***, IEEE Trans. Microwave Theory Tech.***, Vol. 36, No. 12, (1988), 1775-1787.
11. Reineix, A. and Jecko, B., "Analysis of Microstrip Patch Antennas Using Finite Difference Time Domain Method", ***IEEE Trans. Antennas Propagat.***, Vol. 37, No. 11, (1989), 1361-1369.
12. Maloney, J. G., Smith, G. S. and Scott JR., W.R., "Accurate Computation of the Radiation from Simple Antennas Using the Finite-Difference Time-Domain Method", ***IEEE Trans. Antennas Propagat.***, Vol. 38, No. 7, (1990), 1059-1068.
13. Maloney, J. G. and Smith, G. S.,"A Study of Transient Radiation from the Wu-King Resistive Monopole—FDTD Analysis and Experimental Measurements", ***IEEE Trans. Antennas Propagat.***, Vol. 41, No. 5, (1993), 668-676.
14. Maloney, J. G. and Smith, G. S., "Optimization of a Conical Antenna for Pulse Radiation: An Efficient Design Using Resistive Loading", ***IEEE Trans. Antennas Propagat.***, Vol. 41, No. 7, (1993), 940-947.
15. Montoya, T. P. and Smith, G. S., "A Study of Pulse Radiation from Several Broad-Band Monopoles", ***IEEE Trans. Antennas Propagat.***, Vol. 44, No. 8, (1996), 1172-1182.
16. Hertel, J. W. and Smith, G. S., "The Insulated Linear Antenna", ***IEEE Trans. Antennas Propagat.***, Vol. 48, No. 6, (2000), 914-920.
17. Shum, S. M. and Luk, K. M., "Characteristics of Dielectric Ring Resonator Antenna with an Air Gap", ***Electronics Letters,*** Vol. 30, No. 4, (1994), 277-278.
18. Shum, S. M. and Luk, K. M.,"Stacked Annular Ring Dielectric Resonator Antenna Excited by

Axi-Symmetric Coaxial Probe"**,** ***IEEE Trans. Antennas Propagat.***, Vol. 43, No. 8, (1995), 889-892.
19. Gangi, A. F., Sensiper, S. and Dunn, G. R., "The Characteristics of Electrically Short, Umbrella Top-Loaded Antennas", ***IEEE Trans. Antennas Propagat.***, Vol. AP-13, (1965), 864-871.
20. Morgan, M. A. and Schwering, F. K., "Eigenmode Analysis of Dielectric Loaded Top-Hat Monopole Antennas", ***IEEE Trans. Antennas Propagat.***, Vol. 42, No. 1, (1994), 54-61.
21. Francavilla, L. A., Mclean, J. S., Foltz, H. D. and Crook, G. E., "Mode–Matching Analysis of Top-Hat Monopole Antennas Loaded with Radially Layered Dielectric", ***IEEE Trans. Antennas Propagat.***, Vol. 47, No. 1, (1999), 179-185.